Differentiating between crop and soil effects on soil moisture dynamics

Helen Scholz[1], Gunnar Lischeid[2,3], Lars Ribbe[1], Ixchel Hernandez Ochoa[4], Kathrin Grahmann[2]

[1]Institute for Technology and Resources Management in the Tropics and Subtropics (ITT), TH Köln, Cologne, Germany
[2]Leibniz Centre for Agricultural Landscape Research (ZALF), Müncheberg, Germany
[3]Institute for Environmental Sciences and Geography, University of Potsdam, Potsdam, Germany
[4]Institute of Crop Science and Resource Conservation (INRES), Crop Science Group, University of Bonn, Bonn, Germany

Correspondence to: kathrin.grahmann@zalf.de

Abstract. There is urgent need for developing sustainable agricultural land use schemes. On the one side, climate change is expected to increase drought risk as well as the frequency of extreme precipitation events in many regions. On the other side, crop production has induced increased greenhouse gas emissions and enhanced nutrient and pesticide leaching to groundwater and receiving streams. Consequently, sustainable management schemes require sound knowledge of site-specific soil hydrological processes, accounting explicitly for the interplay between soil heterogeneities and crops. ~~Here we present a powerful diagnostic tool applied to a highly diversified arable field with seven different crops and two management schemes. A principal component analysis was applied to a set of 64 soil moisture time series.~~ In this study, we apply a principal component analysis ~~robust diagnostic tool~~ to ~~a~~ a ~~a~~ set of 64 soil moisture time series from a diversified cropping field featuring seven distinct crops and two weeding management strategies~~, employing principal component analysis on a dataset of 64 soil moisture time series~~.

About 97% of the spatial and temporal variance of the data set was explained by the first five principal components. Meteorological drivers accounted for 72.3% of the variance,~~. Another~~ 17.0% was attributed to different seasonal behaviour of different crops. While ~~T~~the effect of very low soil moisture in deeper layers at the onset of the growing season explained~~and soil texture explained another~~ the third (4.1%)~~, and soil texture~~ and fourth (2.2%) principal component explained effects of soil texture and cropping schemes on soil moisture ~~of the~~ variance~~, respectively.~~, respectively, the effect of soil depth was ~~The fifth component~~ represented ~~the effect of soil depth~~by the fifth component (1.7%). ~~In contrast~~However, neither topography nor weed control had a significant effect on soil moisture variance. Contrary to common expectations, soil and rooting pattern heterogeneity seemed not to play a major role ~~in this case study~~. Findings of this study highly depend on local conditions. However, we consider the presented approach generally applicable to a large range of site conditions.

1 Introduction

Agriculture plays a major role to ensure the provision of food to~~for~~ a growing global population. At the same time, climate change is putting yield stability at risk due to extreme weather events, rising ~~and is increasing~~ the need for sustainable management of resources, such as water and soil (Trnka et al., 2014). As part of the adaptation to more challenging conditions,

the transformation from large homogeneously cropped fields towards diversified agricultural landscape was identified not only to have positive effects on multiple ecosystem services (Tamburini et al., 2020), but also on the system's resilience to climatic extremes (Birthal and Hazrana, 2019). Additionally, crop diversification is highly beneficial by reducing soil erosion through permanent soil cover (Paroda et al., 2015), and by improving resource use efficiency through wider crop rotations (Rodriguez et al., 2021). In terms of soil water dynamics, crop and management diversification can lead to improved water-stable macro-aggregation, reduced soil compaction and increased soil organic carbon ~~(Karlen et al., 2006)~~ from which soil water infiltration and retention can be positively affected (Alhameid et al., 2020; Fischer et al., 2014; Karlen et al., 2006; Koudahe et al., 2022; Nunes et al., 2018).

However, as the ~~complexity~~ diversity of ~~the~~ independent variables in agricultural systems increases ~~due to diversification measures, so does the complexity of the assessment and monitoring what makes the use of digital technologies indispensable~~ demands for frequency and spacing of soil moisture measurements and related data interpretation grow. Therefore, soil sensing networks are receiving increased attention, particularly in ~~in various fields (Bogena et al., 2022) and are considered as a crucial tool in~~ Precision Agriculture (PA) (Bogena et al., 2022; ~~(~~Salam and Raza, 2020), where the main goal is to~~. The main goal of PA is to~~ increase efficiency and productivity at the farm level, while ~~and at the same time~~ minimizing~~ing~~ the negative impacts on the environment (Taylor and Whelan, 2010). Soil sensor networks can meaningfully contribute to PA~~play a vital role in achieving that~~ as they can be ~~and are~~ used for various purposes, including~~such as for supporting~~ the delineation of management zones (Khan et al., 2020; Salam and Raza, 2020). ~~Though~~ Still, o~~O~~ne of the most important demands to be fulfilled by soil sensing networks ~~, however,~~ is soil moisture monitoring, as ~~. Ac~~accurate measurement of soil water content can play~~will play~~ an important role in improving ~~crop yields and~~ water management and therefore, crop yields (Salam, 2020).

Wireless solutions, for instance based on LoRaWAN (Long Range Wide Area Network) technology, in combination with electromagnetic soil moisture sensors ~~Time Domain Reflectometry (TDR) sensors~~ avoid labour-intensive and destructive soil moisture measurements that disrupt field traffic. The development of such wireless soil monitoring networks enables broad and affordable application also in areas with low cellular coverage (Cardell-Oliver et al., 2019; Lloret et al., 2021; Placidi et al., 2021; Prakosa et al., 2021).

The evolvement of such systems does not only have benefits for management but is also of high relevance for fostering the understanding of hydrological dynamics in the vadose zone. High-resolution datasets measured under real farming conditions can be used to characterize and analyse spatio-temporal dynamics of soil water. Due to the large size of data sets that are recorded with ~~novel~~ wireless sensor networks, sophisticated data analysis approaches are required to detect hidden patterns and determine influence factors on soil moisture variability (Vereecken et al., 2014). Methods include geostatistical analysis ~~approaches, such as soil moisture variograms~~ (Vereecken et al., 2014) or data driven approaches (Hong et al., 2016). With the introduction of multiple-points geostatistics, it became possible to~~-~~ not only analyse patterns but also connect them with factors affecting soil moisture, such as topography, texture, crop growth and water uptake, and land management (Brocca et al., 2010; Strebelle et al., 2003). Wavelet analysis can analyse both localized features as well as spatial trends through which non-stationary variation of soil properties can be considered (Si, 2008). Cross-correlation analysis allowed linking soil moisture

variability to climatic variables (Mahmood et al., 2012). Furthermore, temporal stability analyses detect spots in the investigated area which are consistently wetter or drier than the mean soil moisture (Baroni et al., 2013; Vachaud et al., 1985, Vanderlinden et al., 2012)~~(Baroni et al., 2013)~~. This method was already successfully used to detect soil moisture patterns related to soil properties, vegetation, and topography (Zhao et al., 2010).

Principal component analysis (PCA) is another method that was successfully applied for soil moisture variability analysis at the field (Hohenbrink et al., 2016; Hohenbrink and Lischeid, 2015; Martini et al., 2017), catchment (Korres et al., 2010; Lischeid et al., 2017; Nied et al., 2013), and regional (Joshi and Mohanty, 2010) scale. These studies build on previous applications in climatology where the term "Empirical Orthogonal Functions" is used (Bretherton et al., 1992). Space and time dimensions can be disentangled and be assigned to influencing factors. Additionally, the propagation of hydrological signals (e.g. precipitation events) over depth can be assessed (Hohenbrink et al., 2016). This opens up great opportunities for contributing to the knowledge of changing soil-hydrological dynamics in ~~agriculture, especially~~ complex diversified agricultural systems with increasing heterogeneity and site-specific adjustment of crops, soil types and field management ~~of highly diversified fields that~~ which, to our knowledge, ~~-~~ have hardly been studied so far ~~so far~~.

We analysed a high-resolution soil moisture data set measured by a novel underground LoRaWAN monitoring system with TDR sensors in different depths of the vadose zone at a spatial-temporally diversified agricultural field in Northeast Germany. The novelty of this Internet of underground Things (IouT) soil moisture monitoring network is characterized by its unique on-farm installation environment and the deployment of 180 sensors in up to 0.9~~0~~ ~~c~~m soil depth, allowing ~~for~~ high spatio-temporal resolution wireless data transmission, and enabling conventional farming practices like machinery traffic, tillage and mechanical weeding. The main objective of this study was to identify ~~and quantify~~ the drivers of soil moisture variability ~~within the a highly diversified~~in a~~n~~ diversified cropping field ~~arable field~~ in terms of crop selection, soil type and field management by applying PCA. Special focus was put on ~~the~~ the interpretation of spatial and temporal effects of crop diversification and of soil heterogeneities on soil moisture dynamics.

2 Materials and methods

2.1 Study site

The study site (52°26'51.8"N 14°08'37.7"E, 66-83 m.a.s.l.) is located near the city of Müncheberg in the federal state of Brandenburg in Northeastern Germany. The landscape is classified as a hummocky ground moraine that formed during the last glacial periods. Glacial and interglacial processes as well as subsequent erosion resulted in highly heterogeneous soils (Deumlich et al., 2018), being classified as Dystric Podzoluvisols according to the FAO scheme (Fischer et al., 2008). In the top 0.3 m soil layer, total organic carbon was 0.94% and total nitrogen content was 0.07%, and pH was 6.12. Between January 1991 and December 2020, the mean annual temperature in Müncheberg was 9.6°C, and the mean annual sum of precipitation was 509 mm (DWD Climate Data Center (CDC), 2021).

2.2 Experimental setup

The data collection was carried out from December 2020 until mid of August 2021 in the patchCROP experiment (Grahmann et al, 2021; Donat et al., 2022). ~~It~~ This landscape experiment has been set up to study the multiple effects of cropping system diversification ~~of cropping schemes~~ on ~~yield~~productivity, crop health, soil quality, ~~weed, pests and diseases~~ and biodiversity. To that end, ~~a~~ a cluster analysis was carried out based on soil maps and multi-year (2010 to 2019) yield data to identify high and low ~~productivity~~yield potential zones in the ~~70 ha~~70-ha large field (Donat et al., 2022). Afterwards, single experimental units comprising 30 patches with an individual size of 0.52 ha (72 m ~~×~~x 72 m) each, have been implemented in both, high and low~~following two different~~ yield potential zones ~~with~~ where each of those zones is characterized by varying soil conditions and a site-specific five-year, legume-based crop rotation~~s~~ (Grahmann et al., 2021). The remaining area outside of the 30 patches was planted with winter rye. For the current~~is~~ study, twelve out of 30 patches were considered (Table 1~~Table 1Table 1Table 1Table 1Table 1Table 1Table 1~~). In the cropping season 2020/2021, seven different main crops were grown.~~,~~ ~~F in thoese selected patches. F~~for subsequent data interpretation, crops have been grouped ~~They can be grouped~~ into A) winter crops, B) fallow, followed by summer crops and C) cover crops, followed by summer crops. In seven out of ~~the~~ twelve considered patches, weed control was carried out ~~chemically~~ with herbicide application, referred as ~~, which is in the following entitled as~~ "conventional" pesticide application, while ~~. I~~in the remaining five patches, "reduced" pesticide management was carried out by mainly using mechanical weeding, by harrowing, blind harrowing, and hoeing. O~~, and o~~nly in the case of high weed pressure~~,~~ herbicides were applied. ~~primary weed control was conducted mechanically by harrowing, blind harrowing, and hoeing, and only in the case of high weed pressure, herbicides were applied. This control pattern pesticide management is in the following entitled named as "reduced".~~ Due to the potential impact of mechanical weeding-, i.e., on rainwater infiltration, soil evaporation and topsoil rooting intensity, ~~on soil structure and consequently soil evaporation~~ we differentiate between these modes of weed control.

2.3 Data collection

Soil moisture was recorded by a long-range-wide-area network (LoRaWAN) based monitoring system. In each patch, one ~~LoRaWAN node~~ Dribox box ~~was~~ equipped with a SDI-12 distributer (serial data interface at 1200 baud rate, TBS04, TekBox, Saigon, Vietnam) connected to six TDR-sensors (TDR310H, Acclima, Meridian, USA) and attached to an outdoor remote terminal unit (RTU) fully LoRaWAN compliant ~~(~~(TBS12B: 4+1 channel analogue to SDI-12 interface for 24 Bit A/D conversion of sensor signals, ~~DriBox, Lancashire~~ TekBox, Saigon, Vietnam ~~UK~~) was installed. The Dribox ~~was~~ was deployed at least 0.3 m below ground to allow normal field traffic and soil tillage. The sensors and boxes were installed between August and November 2020. At two georeferenced locations, TDR-sensors were installed in 0.3, 0.6 and 0.9 m depth, respectively, approximately 2 m apart from the ~~node~~ Driboxes in angles between 45° and 60°. Soil sensors at 0.3 m were placed horizontally, while sensors at 0.6 and 0.9 m depth were placed vertically using auger-made tunnels and extension tubes for soil insertion.

Driboxes were autarkic in terms of energy supply, and communication was wireless throughout. Thus no electric cabling except from connections between sensors and Driboxes was needed.

The data were recorded every 20 minutes by the LoRa nodes through a LoRa-WAN Gateway DLOS8 (UP GmbH, Ibbenbüren, Germany) which was equipped with the modem TL-WA7510N (TP Link, Hong Kong, China) to transfer the data to a cloud from where collected data could be accessed directly after the measurement. The time series included in this study covered the period from December 01, 2020, until August 14, 2021 (Appendix A). Precipitation and temperature data (Fig. 1) were obtained from two weather stations located in the Eastern and Western end of the main patchCROP field with a 15 min temporal resolution. Climatic water balance was calculated from precipitation and potential evapotranspiration, both measured at the climate station by the German Weather Service in Müncheberg (DWD Climate Data Center (CDC), 2021).

Furthermore, drone imagery from May 20, 2021, May 31, 2021, and July 06, 2021, was used for vegetation assessment. The drone fixed-wing UAV-based RS eBee platform (SenseFly Ltd., Cheseaux-Lausanne, Switzerland) was operated at noon time and recorded multispectral imagery with a Parrot Sequoia+ camera (green, red, NIR, and red edge bands, spatial resolution of 0.105 m) and thermal imagery of the surface (only on May 31, 2021) with a senseFly Duet T camera with a spatial resolution of 0.091 m (Table 2). The multispectral imagery was processed with Pix4D to obtain the Normalized Difference Vegetation Index (NDVI), following Eq. (1):

$$NDVI = \frac{NIR-Red}{NIR+Red} \quad (1)$$

in which NIR is the intensity of reflected near-infrared light (reflected by vegetation) and Red the intensity of reflected red light (absorbed by vegetation). A digital elevation model with a spatial resolution of 1 m (GeoBasis-DE and LGB, 2021) was used to calculate the slope (ArcGIS 10.7.0; ESRI, 2011) (Table 2).

Manual soil texture analysis by layer was carried out for part of the sensors by using a Pürckhauer soil auger of 1 m length in eight of twelve analysed patches. Manual soil textural class was estimated at the field by applying the protocol "Finger test to determine soil types according to DIN 19682-2 and KA5" (Sponagel et al., 2005). Additionally, representative soil samples were collected and analysed at the laboratory to determine particle size distribution (based on the German particle classification) by using the traditional gravimetric sieving method. To extrapolate the soil particle distribution from the laboratory to the manual soil textural classes, the high and low yield potential laboratory samples were pooled separately and the average soil particle distribution by soil textural class was calculated and assigned to the respective soil layer with that particular soil textural class. The soil texture analysis showed that soil texture variability increased with depth. In the third layer (average bottom depth = 92 cm), the sand and clay share across 133 sampling points varied between 53 % to 94 % and 2 % to 22 %, respectively. Soil sample points were between approximately 0.8m and 2.5m far from sensors. The transferability of texture information from the sampling point to the sensor location was not ensured due to high nugget effects.

Furthermore, manual soil texture analysis data ~~are~~were not available for all analysed patches. Consequently, they were not included into further correlation analysis.

In October 2019, the "Geophilus" soil scanner system (Lueck and Ruehlmann, 2013) was used in the entire field to map electrical resistivity (ERa) of the soil as a proxy for soil texture for the top soil, using reference soil samples to calibrate the readings. The "Geophilus" system is based on sensor fusion of with ERa sensors coupled with a gamma (γ) sensor. Apparent electrical conductivity was measured by pulling one or more sensor pairs mounted on wheels across the field where each pair of sensors measured a different soil depth. Amplitude and phase were measured simultaneously using frequencies from 1 MHz to 1 kHz. Reference soil samples were taken in several points and served as calibration information in order to estimate sand, silt and clay content in the top 0.25 m of soil. A non-linear regression model was applied. The RMSE of sand content (5.7%) was considerably smaller than the standard deviation of the sand content in the first layer from the manual soil texture analysis (11.9%), indicating a satisfactory prediction performance. The γ-sensor was used to minimize uncertainties, being less sensitive to soil moisture than the ERa readings (Bönecke et al., 2021). The estimated sand content in the upper 0.25 m at the study site varied between 69.1% and 81.2% and averaged 79.0% (Table 1~~Table 1Table 1Table 1Table 1Table 1Table 1Table 1~~, Figure 2~~Figure 2Figure 2Figure 2Figure 2Figure 2Figure 2Figure 2~~).

2.4 Data processing

Soil moisture data were available at 20-minute intervals. Transmission failures due to discharged batteries, signal disturbances in sinks after rainfall, patches with a high density of biomass (e.g. maize), and theft of parts of the monitoring system led to data gaps ~~due to technical problems or theft of parts of the monitoring system data~~ that amounted to 81 out of 257 days of the measuring period, which were therefore skipped for the analysis~~. These gaps were not filled.~~. Whereas time series of eight sensors were excluded due to a higher frequency of transmission failures,~~.~~ i~~I~~n total, 64 time series were used for the analysis, and ~~whereas time series of eight sensors were excluded due to frequent a higher frequency ofmalfunctioning transmission failures. A~~ additional ~~short~~ data gaps for single sensors were interpolated linearly. Of all 20,668 interpolated gaps, 96-% were shorter than two hours, 3-% between two and six hours and 1-% longer than six hours. In 26 cases, ~~the~~ gaps exceeded the duration of one day. The interpolation was justified as the differences between the values before and after the gaps were within the measuring accuracy of 1 vol-% of the TDR sensors (Acclima Inc., 2019). To ensure equal weighting for the subsequent analysis all soil moisture time series were z-transformed to unit variance and zero mean each (cf. Hohenbrink and Lischeid, 2015). As a consequence, differences of absolute values were not considered by the further analysis.

2.4 Statistical analysis

To identify common temporal patterns among single time series, the soil moisture data set was analysed by a principal component analysis (PCA). In a first step, PCA decomposes the total variance of a multivariate data set into independent

fractions called principal components (PCs). The number of PCs is the same as the number of time series in the input data set. Each PC consists of eigenvectors (loadings), scores, and eigenvalues. The scores reflect the temporal dynamics. The importance of single principal components for single sites is represented by the loadings of each PC (Jolliffe, 2002; Lehr and Lischeid, 2020). Loadings are the Pearson correlation coefficients of the single time series of the input data set with the scores of each PC, respectively. The eigenvalues of the single PC are proportional to the variance that they explain. The PCs are sorted in descending order of eigenvalues. ~~Since the input data have been z-transformed, eigenvalues greater than one indicate that the respective PC represents pattern which are relevant for more than one of the observed time series~~Eigenvalues greater than one indicate that a PC explains more variance than ~~one~~ a single input time series could contribute to the total variance of the entire input data set~~.~~ (Kaiser, 1960). More details on principal component analysis for time series analysis are found in Joliffe (2002). The PCA was performed using the *prcomp* function in R version 4.1.0 (R Development Core Team, 2021). ~~To filter out local effects or the effect of selected PCs from z-transformed observed time series at a specific location, a multiple linear regression was applied between the respective time series and the remaining PCs (Lehr and Lischeid, 2020).~~

The scores of the principal components constitute time series. Every observed time series can be presented at arbitrary precision as a combination of various principal components. When the data set consists of time series of the same observable measured at different locations, the first principal component describes the mean behaviour inherent in the data set. Subsequent principal components reflect typical modifications of that mean behaviour at single locations due to different effects. ~~Moreover~~Thus~~,~~ generating synthetic time series as linear combinations of the first PC and another additional PC helps to assign this additional PC to a specific effect. To that end, scores of that component have either been added to or subtracted from those of the first component using arbitrarily selected factors. The two resulting graphs show ~~the two extremes in which way~~how the respective~~specific~~ PC ~~can~~ causes deviations from the mean behaviour of the data set. ~~This is applicable in case the eigenvalue of the first PC is considerably higher than the ones of the following PCs and can be therefore seen as a proxy for the mean behaviour of the data set. The higher the arbitrarily factor is, the more extreme the deviations are displayed.~~

The relations to soil and vegetation parameters were tested by computing the Pearson correlation coefficients between the scores and arithmetic mean values of all input time series as well as the Pearson correlation coefficients between loadings and sand content, sensor depth, antecedent z-transformed water contents, slope, and ~~the~~ drone imagery products ~~from May 31, 2021~~ (NDVI and surface temperature). Eventually, the Wilcoxon-Mann-Whitney test was applied to check whether loadings can be grouped by management parameters (crops, cover crops, weeding management).

All statistical analyses were conducted with R version 4.1.0 (R Development Core Team, 2021).

3 Results

The principal component analysis yielded five components with Eigenvalues exceeding one, which accounted for >97% of the total variance of the data set (Table 4).

3.1 First principal component

The first principal component explained 72.3% spatiotemporal variance of the data set. All loadings on the first PC were negative (Appendix B). The Pearson correlation coefficient of the scores of the first principal component with the mean values of all input time series was less than - 0.999 ($p < 0.01$), the correlation between the scores and the cumulative climatic water balance ($P - ET_p$) was -0.969 ($p < 0.01$). Thus, the time series of the negative scores of this component ~~with reversed sign~~ represented the mean behaviour of soil moisture driven by external factors such as precipitation, temperature, and seasons in general which affected time series in the same way, although to different degrees (cf., Hohenbrink et al., 2016; Lischeid et al., 2021).

3.2 Second principal component

The second principal component explained 17.0% of the total variance. The loadings ranged from -0.801 to 0.760 with a median of -0.030 (Figure 3~~Figure 3Figure 3Figure 3Figure 3Figure 3Figure 3Figure 3~~). The loadings showed a crop type specific pattern. All winter crops (barley, oats, rye) had positive loadings with only one exception in 0.9 m depth. The summer crops maize, soy, and sunflower exhibited negative loadings. In contrast, the summer crop lupine exhibited mostly positive loadings, similar to the winter crops, although of slightly smaller magnitude. According to the Wilcoxon-Mann test, the group of barley, oats, rye, and lupine differed significantly from the group of maize, soy, and sunflower.

~~The scores of the principal components constitute time series. Every observed time series can be presented at arbitrary precision as a combination of various principal components. Moreover, generating synthetic time series as linear combinations of the first and the second principal components helps to assign the second principal component to a specific effect. To that end scores of that component have either been added to or subtracted from those of the first component using arbitrarily selected factors~~As described in the ~~methods~~Methods section, synthetic time series were generated ~~by using arbitrarily factors for pointing out how scores of a specific PC deviate from~~as a linear combination of PC1 and PC2 (Figure 4). The graph resulting from a~~A~~pplying a positive factor for PC2 ~~would~~ represents a typical deviation from mean behaviour for sites that exhibit positive loadings, e.g., ~~generates a synthetic time series which beshows typical behavior for~~ winter crops (blue line) ~~which load positively on that component~~. The opposite holds for the summer crops which load negatively with PC2 (orange line). Both lines plot very close to each other in February and March. In contrast, the orange line ~~is underneath~~ shows lower values than the blue line in December and January, indicating lower soil moisture at the summer crop patches. The inverse holds for the subsequent summer period starting in early June, pointing to earlier and more rapid water uptake of the winter crops. In July and August, the approximately constant level of the blue curve indicates that only summer crops continue to consume water while winter crops are in their ripening phase and eventually harvested.

Lupine and sunflower were the summer crops which were sown first (March 30, 2021, and April 2, 2021, respectively). Maize was sown on April 16, 2021, and soy on May 15, 2021. The loadings of lupine, which were rather performing like winter crops

than summer crops, indicated that lupine showed an early onset of intensive evapotranspiration, compared to other summer crops, especially sunflower which was sown at the same time.

For further investigation of the vegetation effect oin PCs, the loadings of PC2 were compared to drone imagery taken atthe end ofon May 31, 2021, when all patches were covered by cropswhen sowing has been completed on all patches, and images taken atby the beginning of July during winter crops' ripening phase. The second PC's loadings of the time series from different sensors were compared to the Normalized Difference Vegetation Index (NDVI) and surface temperature (only available for May 31, 2021) of the respective sensor location as a proxy for actual evapotranspiration (Table 3Table 3Table 3Table 3Table 3Table 3Table 3Table 3Table 3). As shown inAt the end of May, the NDVI, as a proxy for photosynthesis potential, was positively correlated with the loadings. while sSurface temperature exhibited a negative correlation.s, On the other hand tThe spatial pattern of surface temperature is assumed to be inversely related to that of actual evapotranspiration. Thus, both proxies, NDVI and surface temperature, support the inference that positive loadings on this principal component represent sites with above-average plant activity and root water uptake at the end of May. indicating higher evapotranspiration. This holds for sensors from all depths but was the closest for 0.9 m depth (Pearson correlation of r = -0.916 for surface temperature and of r = 0.946 for NDVI on May 31). The results in July compared to those in May support the observation. At the time when the winter crops are already in the ripening phase and the summer crops reach high levels of evapotranspiration, the correlations are being reversed and negative loadings indicate above-average plant activity for summer crops. On July 06, highest Pearson correlations for NDVI are found for 0.6 m depth (r = -0.917).

3.3 Third principal component

The third PC explained 4.1% of the total data set's variance. Loadings ranged between -0.787 and 0.244 with a median of 0.006. Extreme loadings (<- -0.25) were found only for sensors in 0.9 m depth in patches 66, 89, 95 and 102 (Figure 5Figure 5Figure 5Figure 5Figure 5Figure 5Figure 5Figure 5). The location of the patches roughly follows an east-west direction , which, however, cannot be assigned to topography or structures apparent on the topsoil map These patches are located along a line that roughly follows a west-to-east direction (Figure 2). Loadings were closely related to the minima of the z-transformed soil moisture in the period from December to February (r = 0.70). -The most obvious difference between the orange line (negative loading on PC3) and the blue line (positive loading on PC3) during the first half of the study period is that the latter reaches a maximum of soil moisture after rainfall lmuch earlier compared to the former Strong negative loadings on the third principal component imply delayed response to rainstorms and reduced subsequent dehydration (Figure 6).

3.4 Fourth principal component

The fourth PC explained 2.2% of the total data set's variance. The loadings were clustered by treatment crop groups. All fallow patches showed consistent positive loadings while the patches which were covered by winter crops, (treatment group A) showed mainly negative loadings except in patch 95 where the loadings of the two sensors in 0.3 m depth were slightly above zero (Figure 7Figure 7Figure 7Figure 7Figure 7Figure 7Figure 7Figure 7). According to the Wilcoxon-Mann test treatment

group B (fallow, followed by summer crops) differed significantly from group A (winter crops) and C (cover crops, followed by summer crops) whereas there was no significant difference between group A and C. In contrast to ~~treatment~~ crop groups A and B, patches that were covered by the cover crop phacelia during the winter months, did not show one-directional loadings. ~~Besides showing a treatment group pattern, the loadings of PC4 also correlated with the sand content in a 1 m radius around the sensor locations in the upper 0.25 m (r = 0.67). Due to a lack of sand content data for deeper layers, only data from the sensor depth of 0.3 m were analysed. The second best correlation coefficient is found for PC3 with 0.36.~~

Figure 8 illustrates the effect of the fourth PC on time series. A positive factor would be typical for more sandy soils and for patches with fallow in autumn and winter (blue line). In contrast the orange line depicts behaviour in more loamy soils and for winter crops. The latter line exhibits slightly more delayed responses to rainstorms and subsequent less steep recovery as it would be expected for more loamy soils. However, it is not clear how winter crops on the one side and fallow on the other side could induce such a different behaviour.~~. This pattern would be consistent with a lower sand content.~~

3.5 Fifth principal component

The fifth PC explained 1.7% of the data set's variance. The loadings showed a depth-related pattern. All time series from the 0.3 m depth exhibited negative loadings with two minor exceptions. W~~w~~hereas all time series from 0.9 m depth showed positive loadings throughout, and time series from 0.6 m depth plot in between. Loadings in 0.6 m depth and 0.9 m depth were mostly more similar to each other than to the loadings of 0.3 m depth (Figure 9). The Pearson correlation coefficient between loadings and depth was $r = 0.710$ ($p < 0.05$). Thus it can be concluded that the fifth PC reflected the effect of soil depth on soil moisture variance. ~~Note that t~~This effect differed between crops, with~~. T~~ the three most negative loadings ~~were~~ found in maize patches while the three most positive loadings were found in ~~sunflower~~ lupine patches.

The hydrological signal after rainfall events exhibits damping over depth (blue line) while sensors in the upper layer react with a higher sensitivity (orange line) to weather conditions (Figure 10).

Neither patterns in topography nor in weeding management modes were reflected in the loadings of PC1-PC5. Due to the lack of subsurface soil data, no additional findings could be derived from the Geophilus texture analysis.

4 Discussion

The first five principal components described about 97% of the variance of the data set, which consisted of observed time series from 64 soil moisture probes and revealed various effects of weather, ~~. That results pointed to considerable redundancies between the effects of~~ soil texture, soil depth, ~~heterogeneities and of twelve different~~ crops and management schemes (Table 1). ~~Thereof t~~The first principal component captured 72% of the total variance. Consequently, 72% of the observed dynamics could be described by a lumped model that would not consider any within-field heterogeneity. This figure is in the range of similar studies. In the study of Martini et al. (2017), the first PC explained 58% of the variance of a data set that comprised both agricultural fields as well as grassland transects. Lischeid et al. (2017) ascribed 70% of the variance of a forest soil

hydrological data set to a single component. In the study by Hohenbrink et al. (2016), 85% of the variance of soil hydrological data in a set of arable field experiments with two different crop rotation schemes was ~~assigned to a common dynamic.~~attributed to the first principal component.

4.1 Crop effects

As Korres et al. (2015) stated, the main causes for spatial variability of soil moisture in agricultural fields besides soil parameters are vegetation and management (e.g. planting and harvesting dates). The quantification of the impact of these~~se~~ effects on soil moisture variability is highly important, for instance for hydrological applications and adopted management practices in agriculture (Hupet and Vanclooster, 2002). Joshi and Mohanty (2010) investigated the spatial soil moisture variability on the field to regional scale in the Southern Great Plains regions in the US by means of PCA and assessed the effect of vegetation as limited since none of the first seven PC showed strong correlations with vegetation parameters. In Western China, Wang et al. (2019) used a non-linear Granger causality framework and quantified the vegetation effect on soil moisture variability with up to 8.2%.

In this study, conducted at the field scale, around 17% of the total variance was attributed to the vegetation effect. When not considering the temporal component reflected by PC1 and thus only looking at the spatial variability, 61% of the remaining variance (attributed to PC2 to PC64) is caused by the vegetation effect reflected by PC2. Korres et al. (2010) also used PCA to ~~quantify~~idenetify the drivers of spatial variabilit~~i~~y~~es~~ of soil moisture within a cropped area but did not find such a pronounced vegetation effect. In their study more than two thirds of the spatial variability was related to soil parameters and topography. In contrast, the strong influence of vegetation in our study may be due to the high level of crop diversification. Within single crop fields, vegetation effects are observable due to heterogeneous biomass or root development (Brown et al., 2021; Korres et al., 2010), but may be of a lower magnitude compared to fragmented field arrangements with different crops. The high impact of ~~the~~ crop diversification on soil moisture variability is also visible when comparing our results to the results of a field under comparable conditions in the same region with only two crop rotations in which only 3.8 % was explained by the different crop rotations (Hohenbrink et al., 2016). ~~Yang et al. (2015) remarked that the differences in soil moisture between vegetation types with different biomass is profound especially in deeper layers. In this study, however, the decreasing gradient of the explained variance over depth was indicating the opposite. In the first layer, the effect of vegetation caused the highest variance in soil moisture.~~

It needs to be considered that the proportion of the vegetation effect on soil moisture variability does not only vary spatially and over depth, but also over time. Under dry conditions, soil-plant interactions prevail while under moist conditions, percolation behaviour is predominant (Baroni et al., 2013). ~~In our study, the variability of the vegetation effect over time is observable in the temporal development of the scores.~~ The scores are time series and reflect the effect size of a particular process represented by the respective ~~share of a particular~~ PC ~~in the total variability at the respective time step~~. ~~When~~The more the scores of a certain PC deviate from zero during ~~single~~ specific periods, the stronger the respective effect is. ~~are not stable over time but fluctuate, it can be concluded that the share of the effect represented by this PC is also variable over time.~~

~~Therefore,~~ Consequently, the time series ~~temporal variability~~ of PC2 scores indicates that the effect of vegetation on total variabi~~a~~lity varies by time. In accordance with literature, the absolute values of the scores of PC2, representing differences between the contrasting seasonality of crops, are highest in the dry months May to August. In the moist winter months January to March, as well as during the heavy rainfall event in July, the scores of PC2 are relatively small, showing that spatial variability at that time is caused by other factors.

The second principal component clearly differentiated between winter and summer crops, which was driven by the different seasonal patterns of root water uptake (Figure 3~~Figure 3Figure 3Figure 3Figure 3Figure 3Figure 3Figure 3~~). In contrast, the fourth component separated winter crops and fallow (Figure 7~~Figure 7Figure 7Figure 7Figure 7Figure 7Figure 7Figure 7~~). Note that the term "fallow" refers to crop cover in autumn and winter only. Phacelia is grown as a cover crop and usually dies off in frost periods. However, due to rather mild winter temperature this did only partly happen in the study period. Thus some Phacelia patches exhibited negative loadings, similarly to the winter crop patches. Hence the fourth component obviously reflected the effect of plant cover in the winter period, which can hardly be ascribed to different patterns of root water uptake. According to this component, ~~in comparison to soil moisture behaviour of soil not influenced by outside factors,~~ soil moisture dynamics at the fallow patches resembled more the typical behaviour one would expect for~~at of~~ sandy soils, and that of winter crop patches ~~more~~ a more damped behaviour typical ~~for~~of more~~that of~~ loamy soils. That feature could point to a soil carbon effect on the soil's water holding capacity: Only at the winter crop sites organic carbon in soil increased continuously due to root growth and root exudation, whereas mineralisation reduced the organic carbon stock at the fallow sites. Effects of dense living root networks on soil hydraulic conductivity have been reported, e.g., [OB]Scholl et al.~~,~~ (2014), Zhang et al. (2021) and Lange et al. (2013)[OB]. Further soil-vegetation interactions might play a role, such as soil organic matter from cover crops and plant residues (Manns et al., 2014; Rossini et al., 2021). Usually, such effects are assumed to occur only at larger time scales, which is closely related to problems of detecting changes soil organic carbon quantity or quality. So far there is only anecdotal evidence for rather short-term soil organic carbon quality affecting soil hydraulic properties even at smaller time scales. Although this effect constituted only a minor share of soil moisture variance (Table 4), it was clearly discernible as a separate principal component. This effect would be worth to be tested in more detailed studies. If it were to be confirmed, it would be a good example for how ~~plants~~crop management shape~~s~~ soil properties~~their environment.~~.

4.2 Soil texture effects

Texture is another highly important spatial variable that affects soil moisture. The pore size distribution, which is directly linked to texture has great influence on wetting processes as well as on the water retention capacity of soil (Krauss et al., 2010; Rossini et al., 2021). Furthermore, texture influences the evapotranspiration which is another main factor controlling soil moisture (Pan and Peters-Lidard, 2008). For coarse grained soils as they are present in this case study, the water retention capacity is small, resulting in enhanced seepage fluxes (Scheffer and Schachtschabel, 2002; Krauss et al. 2010).

Loadings on the third principal component were not related to crop types. In contrast, a spatial pattern emerged: Only sensors from 0.9 m depth from six adjacent patches exhibited strongly negative loadings (Figure 2), whereas all other sensors showed

minor positive or negative loadings. This points to an effect of subsoil substrates, that is, higher ~~loam~~ clay content and consequently higher water holding capacity. That would be consistent with delayed response to seepage fluxes and reduced desiccation in the vegetation period (Figure 6). Data on the texture at the sensor location in deeper layers would be of high value to confirm the assumptions.

Whereas the third principal component seems to reflect a local peculiarity, the fifth component obviously grasps a more generic feature. Loadings on this component are clearly related with depth (Figure ~~6~~9). Strong positive loadings indicate a strongly damped behaviour of soil moisture time series: The blue line, representing sites with positive loadings on PC5 which is typical for sensors at greater depth (Figure 9), exhibits clearly reduced amplitudes compared to the orange line, that is, sensors at shallow depth (Figure 9, Figure 10). Hohenbrink and Lischeid (2015) combined a hydrological model and principal component analysis to study the effect of soil depth and soil texture on damping of the input signal in more detail. A subsequent field study proved the relevance of that effect in a real-~~-~~world setting (Hohenbrink et al., 2016). Moreover, Thomas et al. (2012) found that damping accounted for a large share of variance in a set of hydrographs from a region of 30,000 km^2. Damping was also the most relevant driver of spatial variance in a set of time series of groundwater head at about the same scale (Lischeid et al., 2021).

5 Conclusion

To disentangle and to quantify different effects of environmental processes in complex settings is a key challenge of agricultural and environmental research. It is an indispensable prerequisite for tailored field and crop management. Mechanistic models are a way to upscale findings from numerous single cause-single effect studies. But there is urgent need to further validate model results and to study interactions between various effects in a systematic way. Principal component analysis is a ~~further~~ step further to meet these challenges although not entirely without problems. In this study which focuses on the interplay between crops and soil heterogeneities in terms of soil moisture dynamics, the strength of the methodology in contributing to disentangling different effects of complex spatially and temporally diversified cropping systems based on a comprehensive real-world data set is presented. More than 97% of the observed spatial and temporal variance was assigned to five different effects. Meteorological drivers explained 72.3% of the total variance. Different seasonal patterns of root water uptake of winter crops compared to summer crops accounted for another 17.0% of variance. An additional share of 2.2% of variance seemed to be related to the effects of a living rooting system on soil hydraulic properties. Heterogeneity of subsoil substrates explained 4.1 % of variance, and the damping effect of input signals in the soil another 1.7%. To summarize, plant-related direct and indirect effects accounted for 19.2% of the variance, and soil-related effects only for 5.8%. In particular, the plant-induced effects on soil hydraulic properties would be worthwhile to be studied in more detail.

Knowledge from data-driven approaches can support ~~A~~adequate crop selection ~~could be~~as a management option to encounter the increasing drought risk in the study region.

It has been shown that principal component analysis has a high value for the application in environmental sciences, as it allows to draw conclusions about variabilities in large data sets from real-world monitoring setups despite gaps in time series. I~~i~~nformation from this study will contribute to elucidate management effects as well as to develop both parsimonious and tailored mechanistic models. Findings of this study highly depend on local conditions. However, we consider the presented approach generally applicable to a large range of site conditions. In this regard, principal component analysis of soil moisture time series performed as a powerful diagnostic tool and is highly recommended.

Acknowledgments

The maintenance of the patchCROP experimental infrastructure and the LoRaWAN soil sensor system is ensured by the Leibniz Centre for Agricultural Landscape Research. The authors acknowledge the additional support from the German Research Foundation under Germany's Excellence Strategy, EXC-2070 – 390732324 – PhenoRob for patchCROP related research activities.

The authors thank Gerhard Kast, Thomas von Oepen, Lars Richter, Robert Zieciak, Sigrid Ehlert and Motaz Abdelaziz for their dedicated support in maintenance of the monitoring system and data collection.

Competing interests

The authors declare that they have no conflict of interest.

References

Acclima Inc.: True TDR310H. Soil-Water-Temperature-BEC-Sensor, 2019.

Alhameid, A., Singh, J., Sekaran, U., Ozlu, E., Kumar, S., and Singh, S.: Crop rotational diversity impacts soil physical and hydrological properties under long-term no- and conventional-till soils, Soil Res., 58, 84, https://doi.org/10.1071/SR18192, 2020.

Baroni, G., Ortuani, B., Facchi, A., and Gandolfi, C.: The role of vegetation and soil properties on the spatio-temporal variability of the surface soil moisture in a maize-cropped field, Journal of Hydrology, 489, 148–159, https://doi.org/10.1016/j.jhydrol.2013.03.007, 2013.

Birthal, P. S. and Hazrana, J.: Crop diversification and resilience of agriculture to climatic shocks: Evidence from India, Agricultural Systems, 173, 345–354, https://doi.org/10.1016/j.agsy.2019.03.005, 2019.

Bogena, H. R., Weuthen, A., and Huisman, J. H.: Recent Developments in Wireless Soil Moisture Sensing to Support Scientific Research and Agricultural Management, Sensors, 22, 9792, https://doi.org/10.3390/s22249792, 2022.

Bönecke, E., Meyer, S., Vogel, S., Schröter, I., Gebbers, R., Kling, C., Kramer, E., Lück, K., Nagel, A., Philipp, G., Gerlach, F., Palme, S., Scheibe, D., Zieger, K., Rühlmann, J.: Guidelines for precise lime management based on high-resolution soil

pH, texture and SOM maps generated from proximal soil sensing data, Precision Agric, 22, 493-523, https://doi.org/10.1007/s11119-020-09766-8, 2021.

Bretherton, C. S., Smith, C., and Wallace, J. M.: An intercomparison of methods for finding coupled patterns in climate data, Journal of Climatology, 5, 541–560, 1992.

Brocca, L., Melone, F., Moramarco, T., and Morbidelli, R.: Spatial-temporal variability of soil moisture and its estimation across scales, Water Resour. Res., 46, https://doi.org/10.1029/2009WR008016, 2010.

Brown, M., Heinse, R., Johnson-Maynard, J., and Huggins, D.: Time-lapse mapping of crop and tillage interactions with soil water using electromagnetic induction, Vadose zone j., 20, https://doi.org/10.1002/vzj2.20097, 2021.

Cardell-Oliver, R., Hübner, C., Leopold, M., and Beringer, J.: Dataset: LoRa Underground Farm Sensor Network, in: Proceedings of the 2nd Workshop on Data Acquisition To Analysis - DATA'19, the 2nd Workshop, New York, NY, USA, 26–28, https://doi.org/10.1145/3359427.3361912, 2019.

Deumlich, D., Ellerbrock, R. H., and Frielinghaus, Mo.: Estimating carbon stocks in young moraine soils affected by erosion, CATENA, 162, 51–60, https://doi.org/10.1016/j.catena.2017.11.016, 2018.

Donat, M., Geistert, J., Grahmann, K., Bloch, R., and Bellingrath-Kimura, S. D.: Patch cropping- a new methodological approach to determine new field arrangements that increase the multifunctionality of agricultural landscapes, Computers and Electronics in Agriculture, 197, 106894, https://doi.org/10.1016/j.compag.2022.106894, 2022.

DWD Climate Data Center (CDC): Historische tägliche Stationsbeobachtungen (Temperatur, Druck, Niederschlag, Sonnenscheindauer, etc.) für Deutschland, Version v21.3, 2021.

Fischer, C., Roscher, C., Jensen, B., Eisenhauer, N., Baade, J., Attinger, S., Scheu, S., Weisser, W. W., Schumacher, J., Hildebrandt, A.: How Do Earthworms, Soil Texture and Plant Composition Affect Infiltration along an Experimental Plant Diversity Gradient in Grassland?, PLos ONE, 9, 6, https://doi.org/10.1371/journal.pone.0098987, 2014.

Fischer, G. F., Nachtergaele, S., Prieler, S., van Velthuizen, H. T., Verelst, L., and Wisberg, D.: Global Agro-ecological Zones Assessment for Agriculture (GAEZ 2008), IIASA, Laxenburg, Austria and FAO, Rome, ~~Italy,~~ 2008.

GeoBasis-DE and Landesvermessung und Geobasisinformation Brandenburg (LGB): Digitales Geländemodell (DGM), Landesvermessung und Geobasisinformation Brandenburg (LGB), Potsdam, ~~Germany,~~ 2021.

Grahmann, K., Reckling, M., Hernandez-Ochoa, I., and Ewert, F.: An agricultural diversification trial by patchy field arrangements at the landscape level: The landscape living lab "patchCROP," in: Aspects of Applied Biology, Intercropping for sustainability: Research developments and their application, 385–391, 2021.

Hohenbrink, T. L. and Lischeid, G.: Does textural heterogeneity matter? Quantifying transformation of hydrological signals in soils, Journal of Hydrology, 523, 725–738, https://doi.org/10.1016/j.jhydrol.2015.02.009, 2015.

Hohenbrink, T. L., Lischeid, G., Schindler, U., and Hufnagel, J.: Disentangling the Effects of Land Management and Soil Heterogeneity on Soil Moisture Dynamics, Vadose Zone Journal, 15, https://doi.org/10.2136/vzj2015.07.0107, 2016.

Hong, Z., Kalbarczyk, Z., Iyer, R. K.: A Data-Driven Approach to Soil Moisture Collection and Prediction, 2016 IEEE International Conference on Smart Computing (SMARTCOMP), St. Louis, MO, USA, 1-6, https://doi.org/10.1109/SMARTCOMP.2016.7501673, 2016.

Hupet, F. and Vanclooster, M.: Intraseasonal dynamics of soil moisture variability within a small agricultural maize cropped field, Journal of Hydrology, 261, 86–101, 2002.

Jolliffe, I. T.: Principal component analysis. Springer Series in Statistics, Springer, New York, 2002.

Joshi, C. and Mohanty, B. P.: Physical controls of near-surface soil moisture across varying spatial scales in an agricultural landscape during SMEX02: Physical controls of soil moisture, Water Resour. Res., 46, https://doi.org/10.1029/2010WR009152, 2010.

Kaiser, H. F.: The Application of Electronic Computers to Factor Analysis, Educ.Psychol. Measur., 20, https://doi.org/10.1177/001316446002000116, 1960.

Karlen, D. L., Hurley, E. G., Andrews, S. S., Cambardella, C. A., Meek, D. W., Duffy, M. D., and Mallarino, A. P.: Crop Rotation Effects on Soil Quality at Three Northern Corn/Soybean Belt Locations, Agron.j., 98, 484–495, https://doi.org/10.2134/agronj2005.0098, 2006.

Khan, H., Farooque, A. A., Acharya, B., Abbas, F., Esau, T. J., and Zaman, Q. U.: Delineation of Management Zones for Site-Specific Information about Soil Fertility Characteristics through Proximal Sensing of Potato Fields, Agronomy, 10, 1854, https://doi.org/10.3390/agronomy10121854, 2020.

Korres, W., Koyama, C. N., Fiener, P., and Schneider, K.: Analysis of surface soil moisture patterns in agricultural landscapes using Empirical Orthogonal Functions, Hydrol. Earth Syst. Sci., 14, 751–764, https://doi.org/10.5194/hess-14-751-2010, 2010.

Korres, W., Reichenau, T. G., Fiener, P., Koyama, C. N., Bogena, H. R., Cornelissen, T., Baatz, R., Herbst, M., Diekkrüger, B., Vereecken, H., and Schneider, K.: Spatio-temporal soil moisture patterns – A meta-analysis using plot to catchment scale data, Journal of Hydrology, 520, 326–341, https://doi.org/10.1016/j.jhydrol.2014.11.042, 2015.

Koudahe, K., Allen, S. C., Djaman, K.: Critical review of the impact of cover crops on soil properties, International Soil and Water Conservation Research, 10, 343-354, https://doi.org/10.1016/j.iswcr.2022.03.003, 2022.

Krauss, L., Hauck, C., and Kottmeier, C.: Spatio-temporal soil moisture variability in Southwest Germany observed with a new monitoring network within the COPS domain, metz, 19, 523–537, https://doi.org/10.1127/0941-2948/2010/0486, 2010.

Lange, B., Germann, P. F., and Lüscher, P.: Greater abundance of Fagus sylvatica in coniferous flood protection forests due to climate change: impact of modified root densities on infiltration, Eur J Forest Res, 132, 151–163, https://doi.org/10.1007/s10342-012-0664-z, 2013.

Lehr, C. and Lischeid, G.: Efficient screening of groundwater head monitoring data for anthropogenic effects and measurement errors, Hydrol. Earth Syst. Sci., 24, 501–513, https://doi.org/10.5194/hess-24-501-2020, 2020.

Lischeid, G., Frei, S., Huwe, B., Bogner, C., Lüers, J., Babel, W., and Foken, T.: Catchment Evapotranspiration and Runoff, in: Energy and Matter Fluxes of a Spruce Forest Ecosystem, vol. 229, Springer, Cham, Cham, 355–375, 2017.

Lischeid, G., Dannowski, R., Kaiser, K., Nützmann, G., Steidl, J., and Stüve, P.: Inconsistent hydrological trends do not necessarily imply spatially heterogeneous drivers, Journal of Hydrology, 596, 126096, https://doi.org/10.1016/j.jhydrol.2021.126096, 2021.

Lloret, J., Sendra, S., Garcia, L., and Jimenez, J. M.: A Wireless Sensor Network Deployment for Soil Moisture Monitoring in Precision Agriculture, Sensors, 21, 7243, https://doi.org/10.3390/s21217243, 2021.

Lueck, E. and Ruehlmann, J.: Resistivity mapping with Geophilus Electricus - Information about lateral and vertical soil heterogeneity, Geoderma, 199, 2–11, https://doi.org/10.1016/j.geoderma.2012.11.009, 2013.

Mahmood, R., Littell, A., Hubbard, K. G., and You, J.: Observed data-based assessment of relationships among soil moisture at various depths, precipitation, and temperature, Applied Geography, 34, 255–264, https://doi.org/10.1016/j.apgeog.2011.11.009, 2012.

Martini, E., Wollschläger, U., Musolff, A., Werban, U., and Zacharias, S.: Principal Component Analysis of the Spatiotemporal Pattern of Soil Moisture and Apparent Electrical Conductivity, Vadose Zone Journal, 16, vzj2016.12.0129, https://doi.org/10.2136/vzj2016.12.0129, 2017.

Nied, M., Hundecha, Y., and Merz, B.: Flood-initiating catchment conditions: a spatio-temporal analysis of large-scale soil moisture patterns in the Elbe River basin, Hydrol. Earth Syst. Sci., 17, 1401–1414, https://doi.org/10.5194/hess-17-1401-2013, 2013.

Nunes, M. R., van Es, H. M., Schindelbeck, R., Ristow, A. J., Ryan, M.: No-till and cropping system diversification improve soil health and crop yield, Geoderma, 328, 30-43, https://doi.org/10.1016/j.geoderma.2018.04.031, 2018.

Pan, F. and Peters-Lidard, C. D.: On the Relationship Between Mean and Variance of Soil Moisture Fields, JAWRA Journal of the American Water Resources Association, 44, 235–242, https://doi.org/10.1111/j.1752-1688.2007.00150.x, 2008.

Paroda, Raj. S., Suleimenov, M., Yusupov, H., Kireyev, A., Medeubayev, R., Martynova, L., and Yusupov, K.: Crop Diversification for Dryland Agriculture in Central Asia, in: CSSA Special Publications, edited by: Rao, S. C. and Ryan, J., Crop Science Society of America and American Society of Agronomy, Madison, WI, USA, 139–150, https://doi.org/10.2135/cssaspecpub32.c9, 2015.

Placidi, P., Morbidelli, R., Fortunati, D., Papini, N., Gobbi, F., and Scorzoni, A.: Monitoring Soil and Ambient Parameters in the IoT Precision Agriculture Scenario: An Original Modeling Approach Dedicated to Low-Cost Soil Water Content Sensors, Sensors, 21, 5110, https://doi.org/10.3390/s21155110, 2021.

Prakosa, S. W., Faisal, M., Adhitya, Y., Leu, J.-S., Köppen, M., and Avian, C.: Design and Implementation of LoRa Based IoT Scheme for Indonesian Rural Area, Electronics, 10, 77, https://doi.org/10.3390/electronics10010077, 2021.

R Development Core Team: R: A Language and Environment for Statistical Computing, R Foundation for Statistical Computing (Version 4.1.0, http://www.R-project.org), Vienna, Austria, 2021.

Rodriguez, C., Mårtensson, L.-M. D., Jensen, E. S., and Carlsson, G.: Combining crop diversification practices can benefit cereal production in temperate climates, Agron. Sustain. Dev., 41, 48, https://doi.org/10.1007/s13593-021-00703-1, 2021.

Rossini, P. R., Ciampitti, I. A., Hefley, T., and Patrignani, A.: A soil moisture-based framework for guiding the number and location of soil moisture sensors in agricultural fields, Vadose zone j., 20, https://doi.org/10.1002/vzj2.20159, 2021.

Salam, A.: Internet of Things for Sustainable Community Development: Wireless Communications, Sensing, and Systems, Springer International Publishing, Cham, Switzerland, https://doi.org/10.1007/978-3-030-35291-2, 2020.

Salam, A. and Raza, U.: Signals in the Soil: Developments in Internet of Underground Things, Springer International Publishing, Cham, Switzerland, https://doi.org/10.1007/978-3-030-50861-6, 2020.

Scheffer, F. and Schachtschabel, P.: Lehrbuch der Bodenkunde, 15th ed., Spektrum Akademischer Verlag GmbH. Berlin, Heidelberg, https://doi.org/10.1007/978-3-662-55871-3, 2002.

Scholl, P., Leitner, D., Kammerer, G., Loiskandl, W., Kaul, H.-P., and Bodner, G.: Root induced changes of effective 1D hydraulic properties in a soil column, Plant Soil, 381, 193–213, https://doi.org/10.1007/s11104-014-2121-x, 2014.

Si, B. C.: Spatial Scaling Analyses of Soil Physical Properties: A Review of Spectral and Wavelet Methods, Vadose Zone Journal, 7, 547–562, https://doi.org/10.2136/vzj2007.0040, 2008.

Sponagel, H., Grottenthaler, W., Hartmann, K.J., Hartwich, R., Janetzko, P., Joisten, H., Kühn, D., Sabel, K.J., Traidl, R. (Eds.): Bodenkundliche Kartieranleitung (German Manual of Soil Mapping, KA5), 5th edition, Bundesanstalt für Geowissenschaften und Rohstoffe, Hannover, 2005.

Strebelle, S., Payrazyan, K., and Caers, J.: Modeling of a Deepwater Turbidite Reservoir Conditional to Seismic Data Using Principal Component Analysis and Multiple-Point Geostatistics, SPE Journal, 8, 227–235, https://doi.org/10.2118/85962-PA, 2003.

Tamburini, G., Bommarco, R., Wanger, T. C., Kremen, C., van der Heijden, M. G. A., Liebman, M., and Hallin, S.: Agricultural diversification promotes multiple ecosystem services without compromising yield, Sci. Adv., 6, eaba1715, https://doi.org/10.1126/sciadv.aba1715, 2020.

Taylor, J. and Whelan, B.: A General Introduction to Precision Agriculture, 2010.

Thomas, B., Lischeid, G., Steidl, J., and Dannowski, R.: Regional catchment classification with respect to low flow risk in a Pleistocene landscape, Journal of Hydrology, 475, 392–402, https://doi.org/10.1016/j.jhydrol.2012.10.020, 2012.

Trnka, M., Rötter, R. P., Ruiz-Ramos, M., Kersebaum, K. C., Olesen, J. E., Žalud, Z., and Semenov, M. A.: Adverse weather conditions for European wheat production will become more frequent with climate change, Nature Clim Change, 4, 637–643, https://doi.org/10.1038/nclimate2242, 2014.

Vachaud, G., Passerat De Silans, A., Balabanis, P., Vauclin, M.: Temporal Stability of Spatially Measured Soil Water Probability Density Function, Soil Science Society of America Journal, 49, 822-828, https://doi.org/10.2136/sssaj1985.03615995004900040006x, 1985.

Vanderlinden, K., Vereecken, H., Hardelauf, H., Herbst, M., Martínez, G., Cosh, M. H., Pachepsky, Y. A.: Temporal Stability of Soil Water Contents: A Review of Data and Analyses, Vadose Zone Journal, https://doi.org/10.2136/vzj2011.0178, 2012.

Vereecken, H., Huisman, J. A., Pachepsky, Y., Montzka, C., van der Kruk, J., Bogena, H., Weihermüller, L., Herbst, M., Martinez, G., and Vanderborght, J.: On the spatio-temporal dynamics of soil moisture at the field scale, Journal of Hydrology, 516, 76–96, https://doi.org/10.1016/j.jhydrol.2013.11.061, 2014.

Wang, Y., Yang, J., Chen, Y., Fang, G., Duan, W., Li, Y., and De Maeyer, P.: Quantifying the Effects of Climate and Vegetation on Soil Moisture in an Arid Area, China, Water, 11, 767, https://doi.org/10.3390/w11040767, 2019.

Yang, L., Chen, L., and Wei, W.: Effects of vegetation restoration on the spatial distribution of soil moisture at the hillslope scale in semi-arid regions, CATENA, 124, 138–146, https://doi.org/10.1016/j.catena.2014.09.014, 2015.

Zhang, J., Li, Y., Yang, T., Liu, D., Liu, X., and Jiang, N.: Spatiotemporal variation of moisture in rooted-soil, CATENA, 200, 105144, https://doi.org/10.1016/j.catena.2021.105144, 2021.

Zhao, Y., Peth, S., Wang, X. Y., Lin, H., and Horn, R.: Controls of surface soil moisture spatial patterns and their temporal stability in a semi-arid steppe, Hydrol. Process., 24, 2507–2519, https://doi.org/10.1002/hyp.7665, 2010.

Figures and Tables

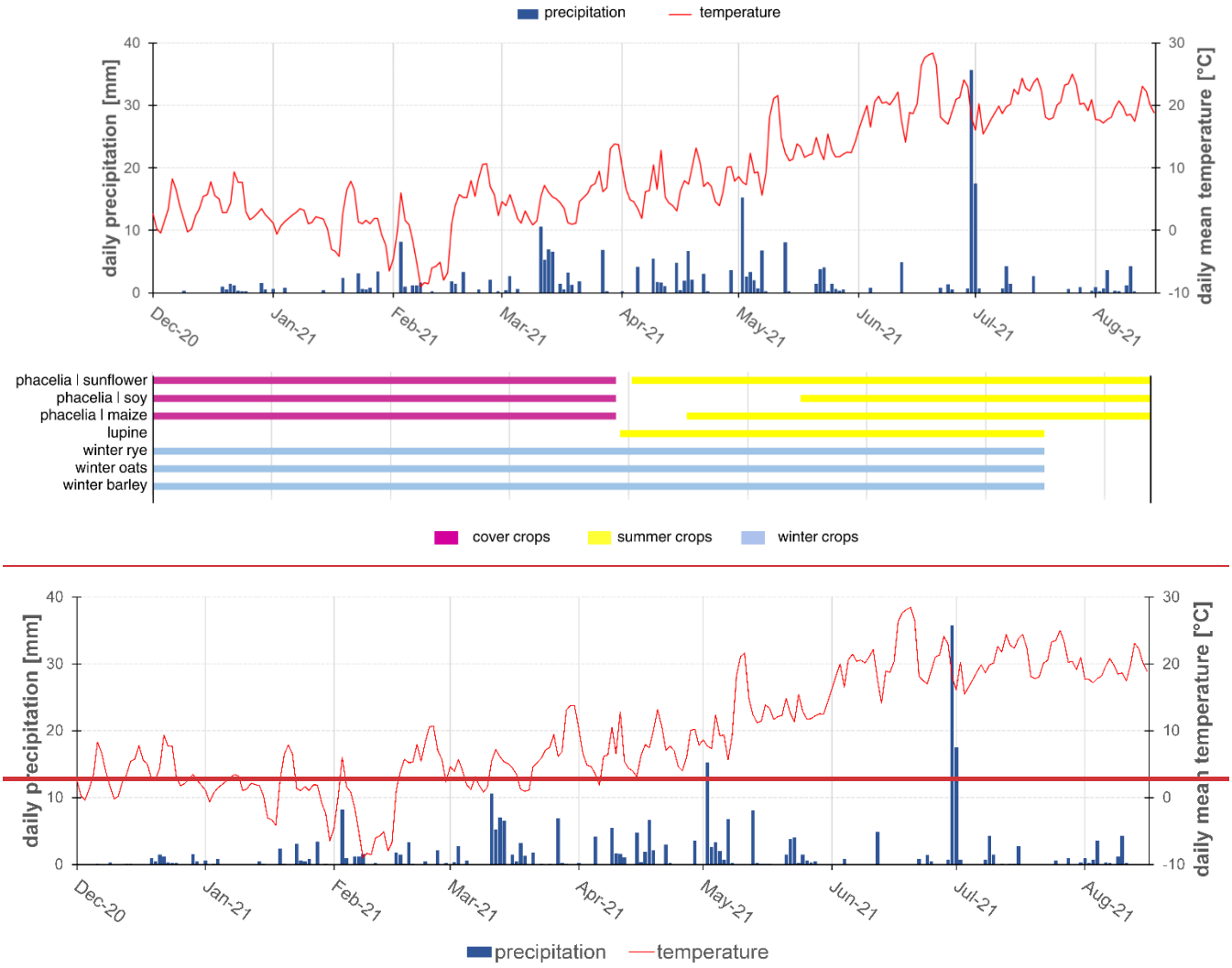

Figure 1: Measured ~~D~~daily precipitation and ~~daily~~ mean temperature and crops grown from 2020-12-01 until 2021-08-15 ~~measured~~ at the experimental site in Tempelberg, Brandenburg, Germany~~the field experiment~~.

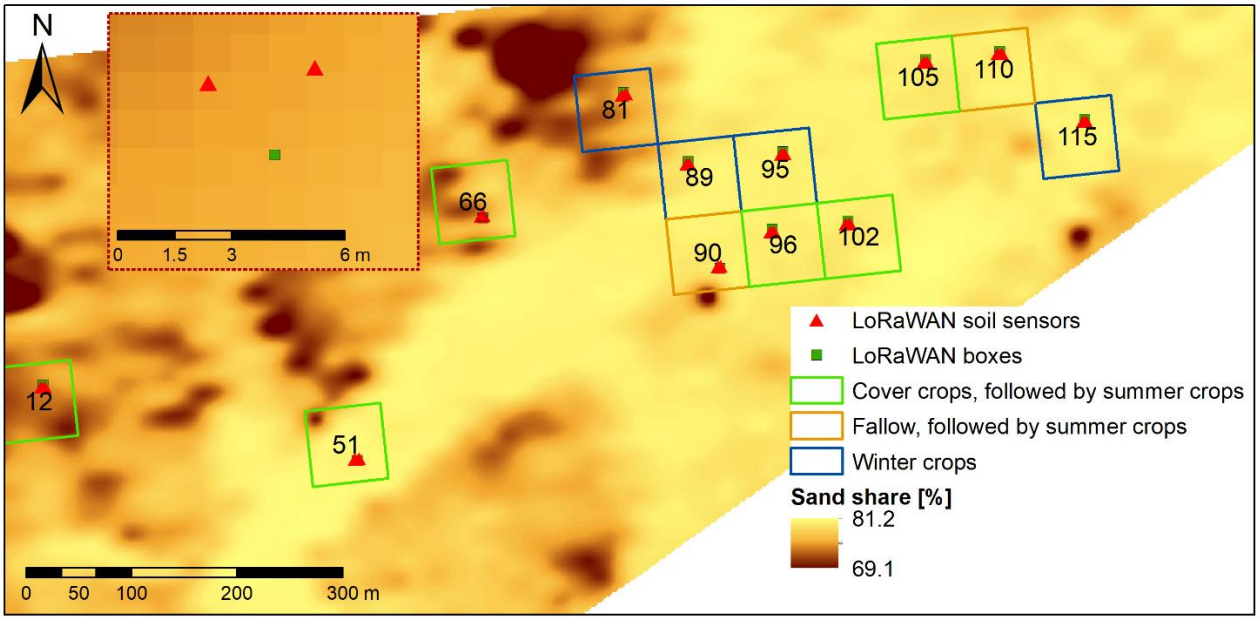

Figure 2: Sand content in the top ~~down to~~ 0.25 m soil depth and location of the analysed patches including soil sensors under different crop rotations in the landscape laboratory patchCROP, Tempelberg, Brandenburg, Germany. The inset shows sensor and box location within one of the patches.

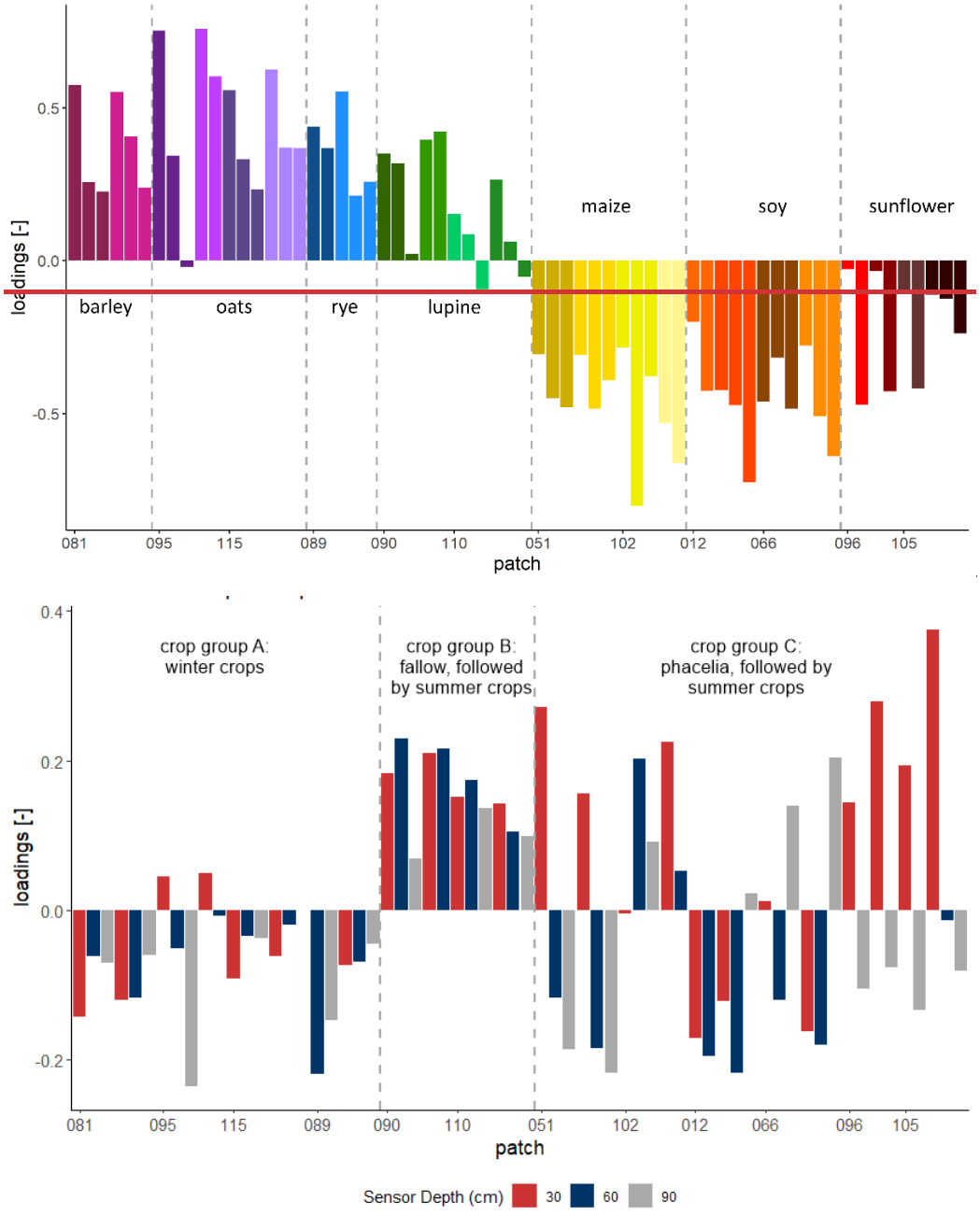

Figure 3: Loadings of time series on the second principal component. Bars represent individual time series grouped by patch ID and sorted by crop~~and coloured by crop~~. ~~Bars of the same colour are sorted by sensor depth, increasing from left to right (0.3 m, 0.6 m, 0.9 m).~~

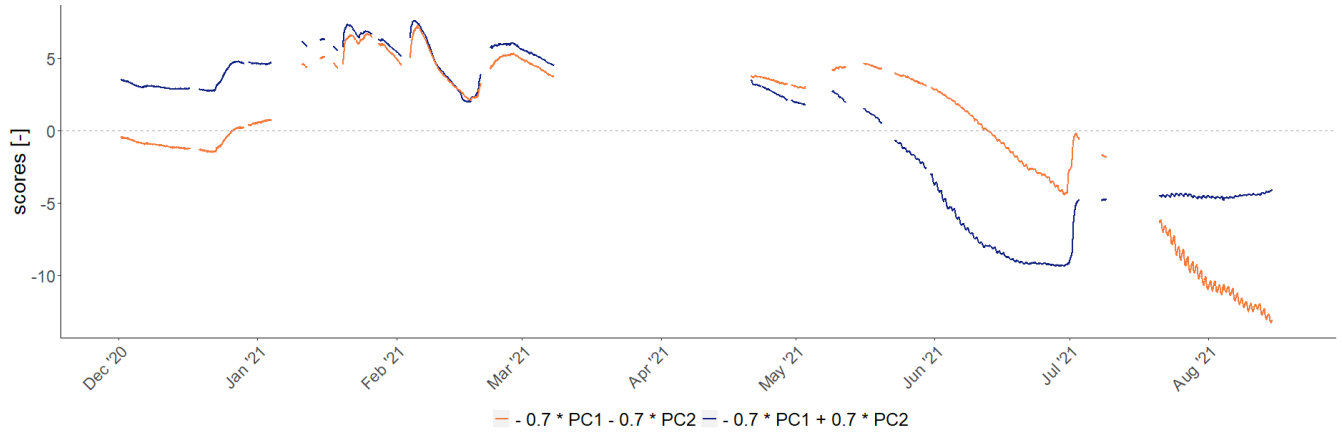

609

610 **Figure 4: Effect of the second principal component on modification of the general mean behaviour which is presented by the first**
611 **principal component.**

612

613

614 **Figure 5: Loadings of time series on the third principal component. Bars represent individual time series grouped by patch ID,**
615 **sorted by crop.**

616

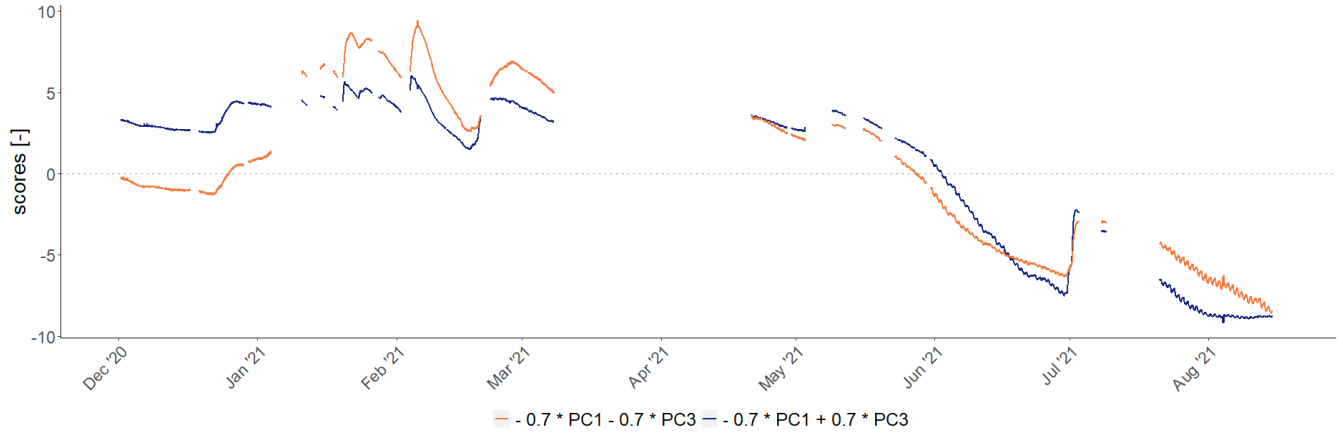

Figure 6: Effect of the third principal component on modification of the general mean behaviour which is presented by the first principal component.

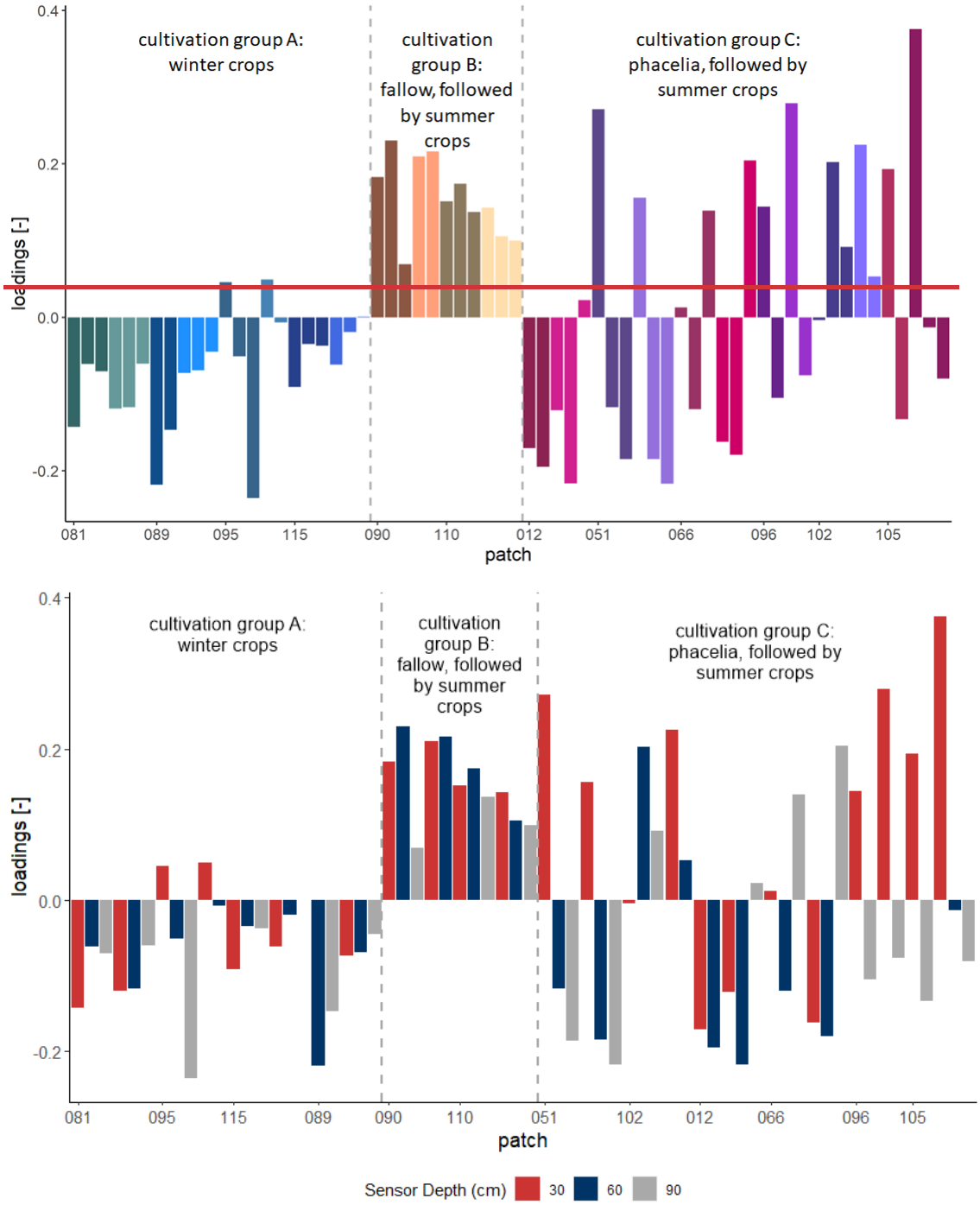

Figure 7: Loadings of time series on the fourth principal component. Bars represent individual time series grouped by patch ID, sorted ~~and coloured~~ by treatment group. ~~Bars of the same colour are sorted by sensor depth, increasing from left to right.~~

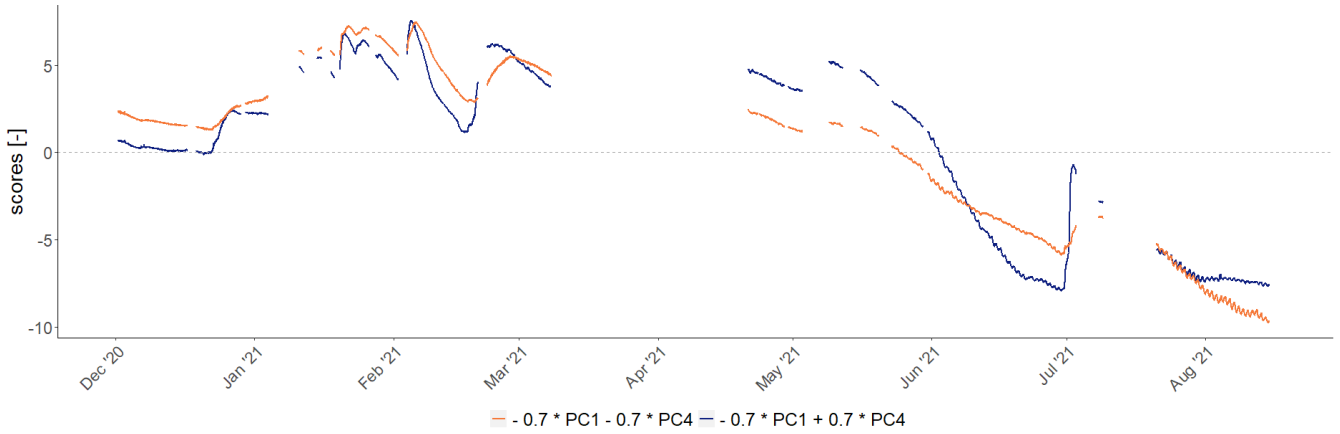

Figure 8: Effect of the fourth principal component on modification of the general mean behaviour which is presented by the first principal component.

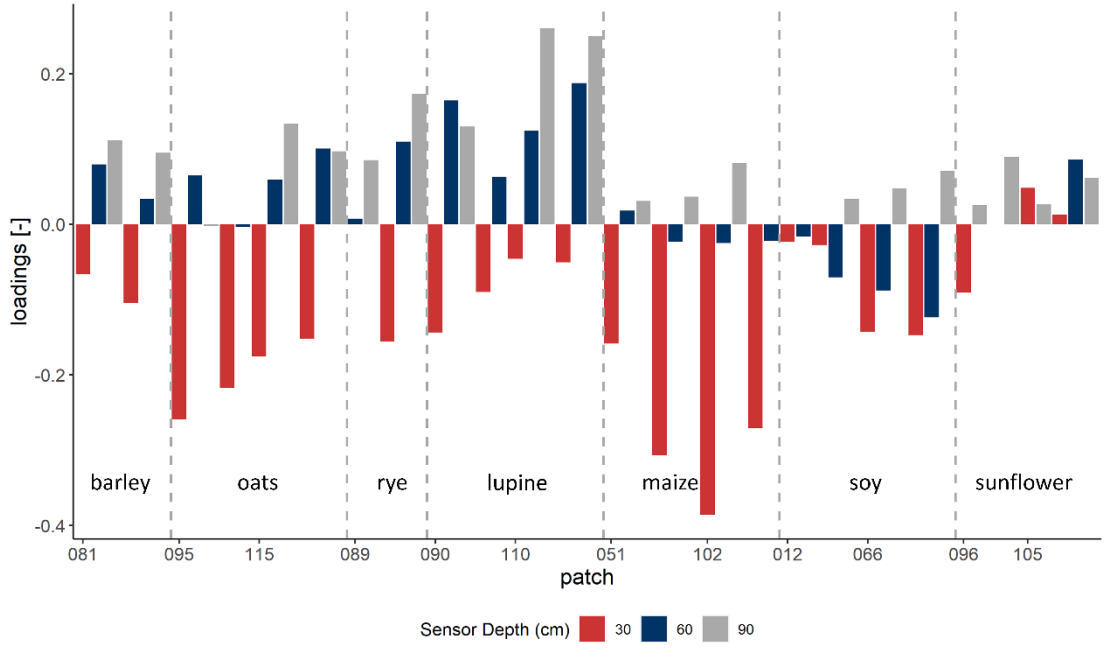

Figure 9: Loadings of time series on the fifth principal component. Bars represent individual time series grouped by patch ID, sorted by crop. ~~**Within each patch, time series are sorted by sensor depth, increasing from left to right.**~~

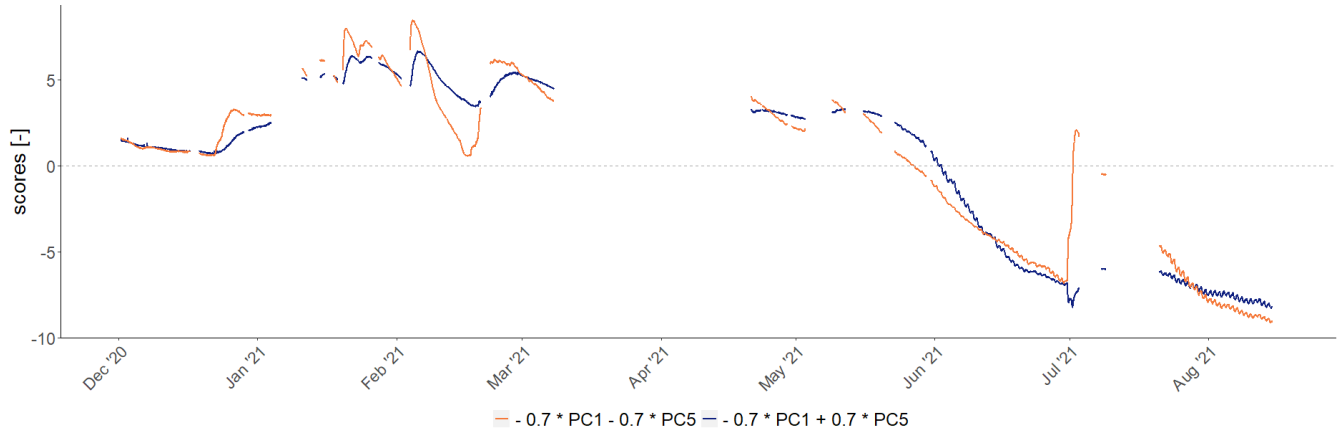

Figure 10: Effect of the fifth principal component on modification of the general mean behaviour which is presented by the first principal component.

Table 1: Overview of crop rotation, sand content in the top ~~down to~~ 0.25 m soil depth and weed control of analysed patches.

Patch ID	Crop in winter season	Crop in ~~growing~~ summer season	~~Treatment~~Crop group	Sand content (in 1 m buffer zone around sensors) [%]	Weed control
81	Winter barley		A	78.3	conventional
~~89~~					
95	Winter oats		A	80.7	conventional
115	Winter oats		A	80.6	reduced
89	Winter rye		A	80.5	conventional
90	Fallow	Lupine	B	80.6	conventional
110	Fallow	Lupine	B	80.3	reduced
51	Phacelia	Maize	C	80.8	reduced
102	Phacelia	Maize	C	80.6	conventional
12	Phacelia	Soy	C	78.5	reduced
66	Phacelia	Soy	C	77.9	conventional
96	Phacelia	Sunflower	C	80.6	conventional
105	Phacelia	Sunflower	C	80.5	reduced

Table 2: Overview of NDVI, surface temperature, ~~both taken on May 31, 2021,~~ and slope at the locations of analysed sensors.

Crop	Patch ID	Sensor Position	NDVI 2021-05-20 [-]	NDVI 2021-05-31 [-]	NDVI 2021-07-06 [-]	Surface Temperature [°C]	Slope [°]

Barley	81	West	0.874	0.182	0.926	20.57	2.01
Barley	81	East	0.875	0.180	0.927	20.43	1.94
Oats	95	East	0.838	0.208	0.834	27.25	1.36
Oats	95	West	0.838	0.213	0.840	27.85	1.15
Oats	115	West	0.756	0.278	0.845	23.70	1.28
Oats	115	East	0.783	0.281	0.863	25.12	0.43
Rye	89	West	0.796	0.263	0.856	22.39	1.74
Rye	89	East	0.787	0.206	0.822	24.95	1.67
Lupine	90	West	0.185	0.395	0.710	26.31	1.40
Lupine	90	East	0.203	0.391	0.733	24.96	1.27
Lupine	110	West	0.090	0.563	0.635	26.98	1.88
Lupine	110	East	0.090	0.567	0.639	26.76	2.50
Maize	51	West	-0.099	0.654	0.181	35.44	0.82
Maize	51	East	-0.096	0.638	0.217	35.29	0.93
Maize	102	West	-0.077	0.714	0.175	37.88	0.88
Maize	102	East	-0.058	0.728	0.178	38.03	0.90
Soy	12	West	-0.107	0.748	0.166	34.87	1.71
Soy	12	East	-0.108	0.723	0.162	34.44	1.11
Soy	66	West	-0.115	0.730	0.144	35.09	2.40
Soy	66	East	-0.114	0.661	0.147	34.39	2.13
Sunflower	96	West	-0.109	0.816	0.211	33.76	0.59
Sunflower	96	East	-0.101	0.827	0.229	34.70	0.69
Sunflower	105	West	0.178	0.610	0.564	29.79	1.04
Sunflower	105	East	0.030	0.696	0.399	34.53	1.00

Table 3: Pearson correlation coefficients between drone imagery products taken on May 31st, 2021, and loadings of sensors in all depths or at single depths, respectively, on the second principal component. All correlations are highly significant (p <0.01).

	Sensors in all depths	0.3 m	0.6 m	0.9 m
Surface temperature	-0.853	-0.881	-0.909	-0.916
NDVI 2021-05-20	~~0.887~~0.836	~~0.9278~~0.904	~~0.934~~0.837	~~0.940~~0.907
NDVI 2021-05-31	0.899	0.945	0.944	0.946

NDVI 2021-07-06	-0.860	-0.898	-0.917	-0.913

Table 4: Principal components 1 to 5.

	PC1	PC2	PC3	PC4	PC5
Eigenvalue	46.25	10.89	2.60	1.43	1.06
Proportion of variance [%]	72.27	17.01	4.06	2.23	1.65
Proportion of variance (cumulative) [%]	72.27	89.28	93.34	95.57	97.22
Interpretation	Mean behaviour	Winter vs. summer crops	Subsoil texture	Soil organic carbon	Damping of the input signal
Prevailing driver	weather	crop	soil	crop and soil	soil

APPENDIX A

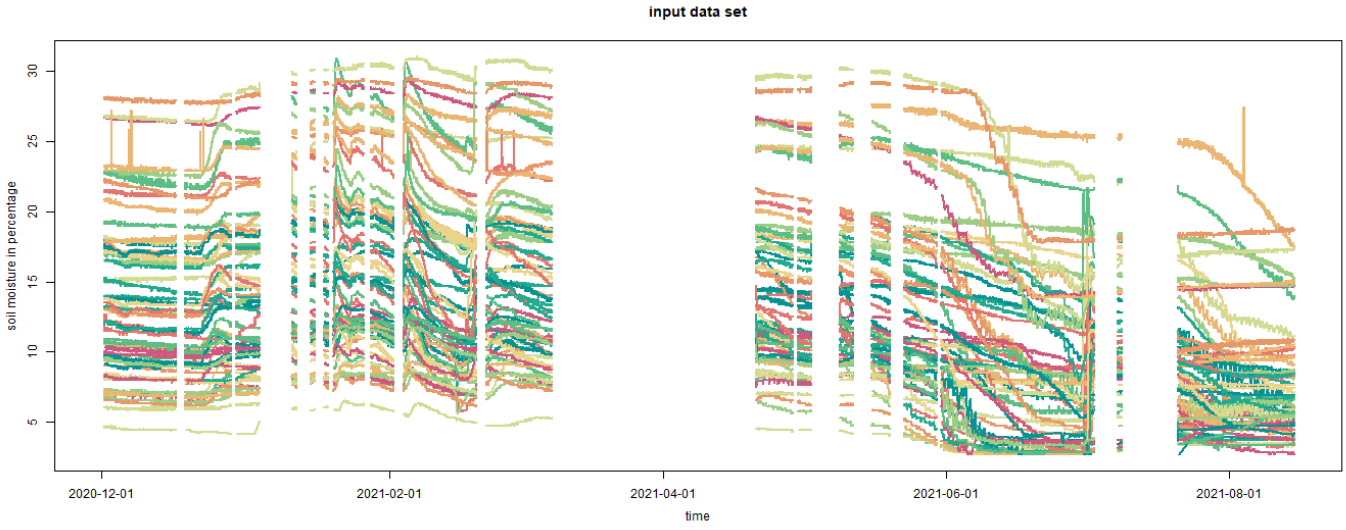

Figure 11: Soil moisture data from 64 sensors in different depths as input data set.

APPENDIX B

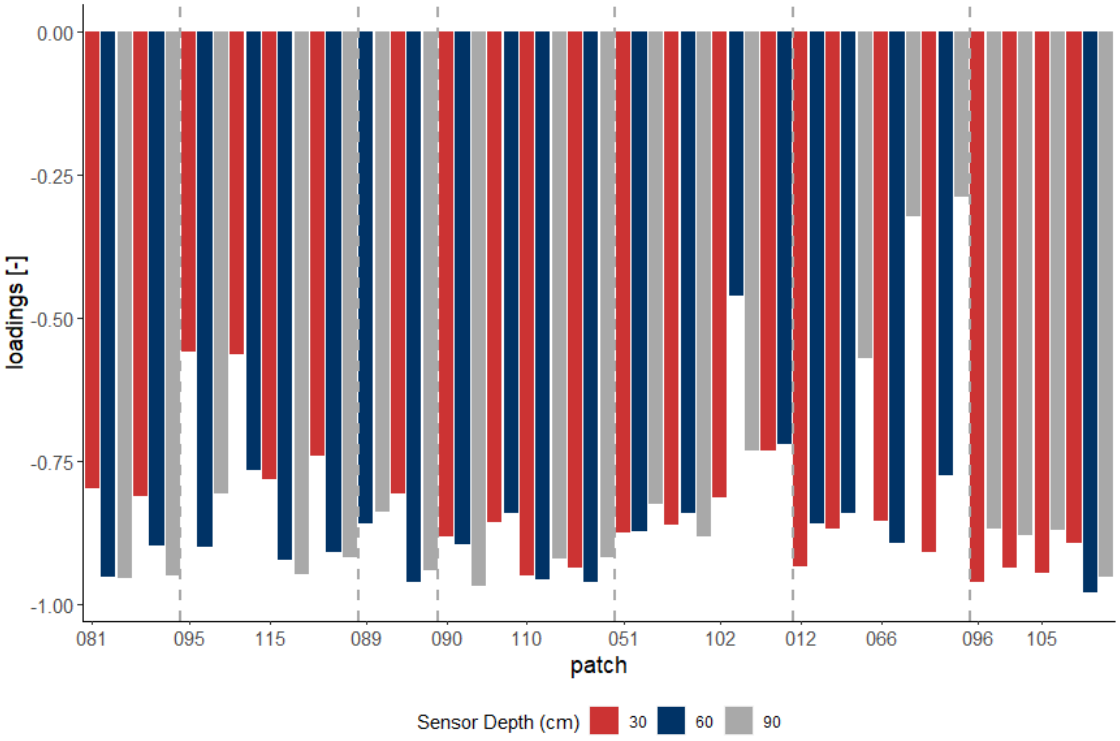

Figure 12: Loadings of time series on the first principal component. Bars represent individual time series grouped by patch ID, sorted by crop. ~~Within each patch, time series are sorted by sensor depth, increasing from left to right.~~